Neutron star moment-of-inertia in the extended Zimanyi-Moszkowski model

K. Miyazaki

E-mail: miyazakiro@rio.odn.ne.jp

Abstract

We revisit the extended Zimanyi-Moszkowski (EZM) model of dense neutron star (NS) core matter. In contrast to our previous work we treat the vector potentials of baryons on an equal footing with the effective masses, and solve a set of 6 equations to determine the three independent effective masses and vector potentials and a set of 2 equations to determine the conditions of β-equilibrated NS matter, simultaneously. According to an expectation that the precisely measurable moment-of-inertia of J0737-3039A will impose a significant constraint on the nuclear equation-of-state (EOS), it is calculated using the two sets of hyperon coupling constants, EZM-SU6 and EZM-P, derived from the SU(6) symmetry and the empirical data of hypernuclei. We find $I_{45} = 1.23$ and 1.64 that are close to the values in the EOSs of "APR" and "MS1" calculated by Morrison *et al.*, while their mass-radius relations are rather different from the EZM models. The uniqueness of the EZM model is also apparent in the correlation map between the maximum gravitational mass of NS and the moment-of-inertia of J0737-3039A calculated for the other 25 EOSs by Bejger *et al.* Consequently, the EZM model is severely tested by the moment-of-inertia. However, whether the model is ruled out or not, there still remain some possibilities and problems of improving it.

1 Introduction

The stiffness of nuclear equation-of-state (EOS) is still a controversial problem in nuclear physics. The kaon production in heavy-ion collisions [1] suggests a soft EOS, while the recent observations of neutron stars (NSs) in RX J1856-3754 [2] and EXO 0748-676 [3] favor a stiff EOS. We are however disturbed by the dependence of the former information on the model of numerical simulation and the uncertainties in the astronomical data. On the other hand, the recently discovered binary NS system J0737-3039 [4-6] is able to provide the detailed tests of general relativity and astrophysics. In a view from the nuclear EOS, it is strongly expected [7-9] that even a moderately accurate measurement of the NS moment-of-inertia will impose a significant constraint on the EOS.

The paper [7] investigated the expectation by means of typical three classes of EOSs for NS matter. The first is based on the nonrelativistic variational calculations, the second is based on the relativistic mean-field (RMF) theory and the third describes the so-called

strange quark star. Although there are large ambiguities in the results of the third class of EOSs, we can see clear differences between the results in the first and second classes. In fact, the EOSs in the first class result in relatively smaller crusts, radii and moments-of-inertia for NSs with $M_G < 1.6M_\odot$ while the EOSs in the second class predict relatively larger values of them.

The paper [8] further investigated 25 EOSs in all. However, the relativistic EOSs in Refs. [7] and [8] are restricted to the so-called nonlinear Walecka (NLW) models [10,11] and their parameters of the self-coupling terms were not physically reasonable. It has been recently shown [12,13] that the NLW model using the reasonable parameters [14] is not useful to dense nuclear system as NS matter. On the other hand, the RMF models with the density-dependent meson-nucleon couplings [15] and the nonlinear couplings are highly promising. In this respect it is also noted that the NLW model is not a truly nonlinear RMF model in spite of its name. The RMF model with the nonlinear meson-nucleon couplings was first developed by Zimanyi and Moszkowski (ZM) [16]. A more elaborate nonlinear model has been recently developed in Ref. [17]. It however includes a lot of parameters and so cannot be applied to hyperons without ambiguities. The density-dependent coupling model [15] has the same defect. To the contrary, the extended Zimanyi-Moszkowski model (EZM) [18-26] developed by the present author is based on the constituent quark model of baryons and so is uniquely applied to strange hadronic matter.

We have already investigated the NS matter within the EZM model in Ref. [23], which takes into account the isoscalar-scalar meson [27] and the hidden strange mesons [28]. There, we first expressed the vector potentials of baryons in terms of the three independent effective masses of proton, neutron and lambda. Then, the two sets of nonlinear equations were solved independently but self-consistently. One set was composed of the three equations to determine the effective masses. Another set was composed of the two equations for the baryon number conservation and the charge neutral condition. As the result we encountered an upper limit of the baryon density above which no β-equilibrium states were found. In the present work we revisit the NS matter in the EZM model by treating the vector potentials on an equal footing with the effective masses. In this case the problem of the limiting density will be resolved. Then, we apply the EZM model to the NS moment-of-inertia.

Because the EZM model is not familiar but has a unique feature, the main purpose of the present paper is to supplement the investigations of Refs. [7] and [8] with the EZM model. The next section reviews the EZM model of NS matter including hyperons. In section 3 we calculate the properties of NS and discuss them in the comparison with the other EOSs. Finally, in section 4 we summarize our investigations and derive conclusions.

2 The EZM model of NS matter

In this work we consider the contributions of the isoscalar mesons σ and ω, their strange counterparts σ^* and ϕ mesons [28] and the isovector mesons [27] δ and ρ. Their masses are taken to be $m_\sigma = 550\,\mathrm{MeV}$, $m_\omega = 783\,\mathrm{MeV}$, $m_{\sigma^*} = 975\,\mathrm{MeV}$, $m_\phi = 1020\,\mathrm{MeV}$, $m_\rho = 769\,\mathrm{MeV}$ and $m_\delta = 983\,\mathrm{MeV}$, respectively. The masses of baryons are assumed to be $M_N = 938.9\,\mathrm{MeV}$, $M_\Lambda = 1115.6\,\mathrm{MeV}$, $M_\Sigma = 1193.05\,\mathrm{MeV}$ and $M_\Xi = 1318.1\,\mathrm{MeV}$, respectively. The Lagrangian of NS matter in the EZM model has the form:

$$\begin{aligned}\mathcal{L} &= \sum_{\substack{B=p,n,\Lambda,\Sigma^+,\\ \Sigma^0,\Sigma^-,\Xi^0,\Xi^-}} \bar{\psi}_B \left(\not{p} - M_B^* - \gamma^0 V_{0B}\right) \psi_B + \sum_{l=e^-,\,\mu^-} \bar{\psi}_l \left(\not{p} - m_l\right) \psi_l \\ &\quad - \frac{1}{2} m_\sigma^2 \langle\sigma\rangle^2 - \frac{1}{2} m_\delta^2 \langle\delta_3\rangle^2 - \frac{1}{2} m_{\sigma^*}^2 \langle\sigma^*\rangle^2 + \frac{1}{2} m_\omega^2 \langle\omega_0\rangle^2 + \frac{1}{2} m_\rho^2 \langle\rho_{03}\rangle^2 + \frac{1}{2} m_\phi^2 \langle\phi_0\rangle^2 ,\end{aligned} \tag{1}$$

where ψ_B and ψ_l are the Dirac fields of baryons and leptons, $\langle\sigma\rangle$, $\langle\omega_0\rangle$, $\langle\delta_3\rangle$, $\langle\rho_{03}\rangle$, $\langle\sigma^*\rangle$ and $\langle\phi_0\rangle$ are the mean-fields. The energy density is

$$\begin{aligned}\mathcal{E} &= \frac{1}{4}\sum_B \left(3E_{FB}^* \rho_B + M_B^* \rho_{SB}\right) + \frac{1}{4}\sum_l \left(3E_{Fl}\rho_l + m_l \rho_{Sl}\right) + \sum_B V_{0B}\rho_B \\ &\quad + \frac{1}{2} m_\sigma^2 \langle\sigma\rangle^2 + \frac{1}{2} m_\delta^2 \langle\delta_3\rangle^2 + \frac{1}{2} m_{\sigma^*}^2 \langle\sigma^*\rangle^2 - \frac{1}{2} m_\omega^2 \langle\omega_0\rangle^2 - \frac{1}{2} m_\rho^2 \langle\rho_{03}\rangle^2 - \frac{1}{2} m_\phi^2 \langle\phi_0\rangle^2 ,\end{aligned} \tag{2}$$

where ρ_B and ρ_l are the vector densities of baryons and leptons in NS matter, ρ_{SN} and ρ_{Sl} are their scalar densities, and E_{FN}^* and E_{Fl} are the Fermi energies.

The effective mass M_B^* of a baryon B in baryon matter is

$$M_B^* = m_B^* M_B = M_B + S_B. \tag{3}$$

Using the renormalized meson-baryon coupling constant $g_{BB\sigma}^*$ etc., the scalar potential S_B is given by

$$S_B = -g_{BB\sigma}^* \langle\sigma\rangle - g_{BB\delta}^* \langle\delta_3\rangle I_{3B} - g_{BB\sigma^*}^* \langle\sigma^*\rangle , \tag{4}$$

where $I_{3B} = \{\,1, -1,\, 0, 1, 0, -1, 1, -1\,\}$ for $B = \{\,p, n, \Lambda, \Sigma^+, \Sigma^0, \Sigma^-, \Xi^0, \Xi^-\}$. On the other hand, the vector potential V_{0B} is given by

$$V_{0B} = g_{BB\omega}^* \langle\omega_0\rangle + g_{BB\rho}^* \langle\rho_{03}\rangle I_{3B} + g_{BB\phi}^* \langle\phi_0\rangle . \tag{5}$$

The scalar mean-fields are expressed [23] in terms of the three independent effective masses of p, n and Λ:

$$\bar{\sigma}_N = \frac{\left(1 - m_p^*\right) g_{nn\delta}^* + \left(1 - m_n^*\right) g_{pp\delta}^*}{D_{SN}}\, g_{NN\sigma}, \tag{6}$$

$$\bar{\delta}_N = \frac{\left(m_n^* - 1\right) g_{pp\sigma}^* - \left(m_p^* - 1\right) g_{nn\sigma}^*}{D_{SN}} \, g_{NN\delta}, \tag{7}$$

$$\bar{\sigma}_\Lambda^* = \frac{2\left(1 - m_\Lambda^*\right) - \left[2 - \frac{1}{2}\left(1 - m_\Lambda^*\right)\right] \bar{\sigma}_\Lambda}{2 - \frac{1}{2}\left(2 + m_\Lambda^*\right) \bar{\sigma}_\Lambda}, \tag{8}$$

where

$$D_{SN} = g_{pp\sigma}^* \, g_{nn\delta}^* + g_{nn\sigma}^* \, g_{pp\delta}^*, \tag{9}$$

and we have introduced the reduced scalar mean-fields for each baryon,

$$\bar{\sigma}_B \equiv \frac{g_{BB\sigma}}{M_B} \left\langle \sigma \right\rangle, \tag{10}$$

$$\bar{\delta}_B \equiv \frac{g_{BB\delta}}{M_B} \left\langle \delta_3 \right\rangle, \tag{11}$$

$$\bar{\sigma}_Y^* \equiv \frac{g_{YY\sigma^*}}{M_Y} \left\langle \sigma^* \right\rangle. \tag{12}$$

The effective masses of Σ and Ξ are given [23] by

$$m_{\Sigma^+}^* = \frac{2 - (3/2)\left(\bar{\sigma}_\Sigma + \bar{\delta}_\Sigma\right) - 2\,\bar{\sigma}_\Sigma^* + \left(\bar{\sigma}_\Sigma + \bar{\delta}_\Sigma\right)\bar{\sigma}_\Sigma^*}{D_{S\Sigma^+}}, \tag{13}$$

$$m_{\Sigma^0}^* = \frac{2 - (3/2)\,\bar{\sigma}_\Sigma - 2\,\bar{\sigma}_\Sigma^* + \bar{\sigma}_\Sigma \bar{\sigma}_\Sigma^*}{D_{S\Sigma^0}}, \tag{14}$$

$$m_{\Sigma^-}^* = \frac{2 - (3/2)\left(\bar{\sigma}_\Sigma - \bar{\delta}_\Sigma\right) - 2\,\bar{\sigma}_\Sigma^* + \left(\bar{\sigma}_\Sigma - \bar{\delta}_\Sigma\right)\bar{\sigma}_\Sigma^*}{D_{S\Sigma^-}}, \tag{15}$$

$$m_{\Xi^0}^* = \frac{2 - 2\left(\bar{\sigma}_\Xi + \bar{\delta}_\Xi\right) - (3/2)\,\bar{\sigma}_\Xi^* + \left(\bar{\sigma}_\Xi + \bar{\delta}_\Xi\right)\bar{\sigma}_\Xi^*}{D_{S\Xi^0}}. \tag{16}$$

$$m_{\Xi^-}^* = \frac{2 - 2\left(\bar{\sigma}_\Xi - \bar{\delta}_\Xi\right) - (3/2)\,\bar{\sigma}_\Xi^* + \left(\bar{\sigma}_\Xi - \bar{\delta}_\Xi\right)\bar{\sigma}_\Xi^*}{D_{S\Xi^-}}, \tag{17}$$

where

$$D_{S\Sigma^+} = 2 + \frac{1}{2}\left(1 - \bar{\sigma}_\Sigma^*\right)\left(\bar{\sigma}_\Sigma + \bar{\delta}_\Sigma\right), \tag{18}$$

$$D_{S\Sigma^0} = 2 + \frac{1}{2}\left(1 - \bar{\sigma}_\Sigma^*\right)\bar{\sigma}_\Sigma, \tag{19}$$

$$D_{S\Sigma^-} = 2 + \frac{1}{2}\left(1 - \bar{\sigma}_\Sigma^*\right)\left(\bar{\sigma}_\Sigma - \bar{\delta}_\Sigma\right), \tag{20}$$

$$D_{S\Xi^0} = 2 + \frac{1}{2}\left[1 - \left(\bar{\sigma}_\Xi + \bar{\delta}_\Xi\right)\right]\bar{\sigma}_\Xi^*, \tag{21}$$

$$D_{S\Xi^-} = 2 + \frac{1}{2}\left[1 - \left(\bar{\sigma}_\Xi - \bar{\delta}_\Xi\right)\right]\bar{\sigma}_\Xi^*. \tag{22}$$

Because $\bar{\sigma}_Y$, $\bar{\delta}_Y$ and $\bar{\sigma}_Y^*$ are expressed by m_p^*, m_n^* and m_Λ^*, the effective masses m_Y^* ($Y \neq \Lambda$) are also expressed by them.

The vector mean-fields are determined from the three independent vector potentials

of p, n and Λ:

$$\langle\omega_0\rangle = \frac{g^*_{nn\rho}V_{0p} + g^*_{pp\rho}V_{0n}}{C_{VN}}, \tag{23}$$

$$\langle\rho_{03}\rangle = \frac{g^*_{nn\omega}V_{0p} - g^*_{pp\omega}V_{0n}}{C_{VN}}, \tag{24}$$

$$\langle\phi_0\rangle = \frac{g^*_{nn\rho}\left(g^*_{pp\omega}V_\Lambda - g^*_{\Lambda\Lambda\omega}V_p\right) + g^*_{pp\rho}\left(g^*_{nn\omega}V_\Lambda - g^*_{\Lambda\Lambda\omega}V_n\right)}{g^*_{\Lambda\Lambda\phi}C_{VN}}, \tag{25}$$

where

$$C_{VN} = g^*_{pp\omega}\, g^*_{nn\rho} + \ g^*_{nn\omega}\, g^*_{pp\rho}. \tag{26}$$

The renormalized coupling constants of nucleons in the above equations are given [19,20] by

$$g^*_{pp\sigma(\omega)} = \left[(1-\lambda_N) + \lambda_N m^*_p\right] g_{NN\sigma(\omega)}, \tag{27}$$

$$g^*_{nn\sigma(\omega)} = \left[(1-\lambda_N) + \lambda_N m^*_n\right] g_{NN\sigma(\omega)}, \tag{28}$$

$$g^*_{pp\delta(\rho)} = \left[(1-\lambda_N) + \lambda_N \left(2m^*_n - m^*_p\right)\right] g_{NN\delta(\rho)}, \tag{29}$$

$$g^*_{nn\delta(\rho)} = \left[(1-\lambda_N) + \lambda_N \left(2m^*_p - m^*_n\right)\right] g_{NN\delta(\rho)}, \tag{30}$$

where $g_{NN\sigma(\omega,\delta,\rho)}$ is the free coupling constant and $\lambda_N = 1/3$.

The renormalized meson-Λ coupling constants are

$$g^*_{\Lambda\Lambda\sigma(\omega)} = \frac{2-\bar\sigma^*_\Lambda}{D_{S\Lambda}}\, g_{\Lambda\Lambda\sigma(\omega)}. \tag{31}$$

$$g^*_{\Lambda\Lambda\sigma^*(\phi)} = \frac{2-(1/2)\,\bar\sigma_\Lambda}{D_{S\Lambda}}\, g_{\Lambda\Lambda\sigma^*(\phi)}, \tag{32}$$

where

$$D_{S\Lambda} = 2 + \frac{1}{2}\left(1-\bar\sigma^*_\Lambda\right)\,\bar\sigma_\Lambda. \tag{33}$$

The renormalized meson-Σ^0 coupling constants have the same forms as those of Λ:

$$g^*_{\Sigma^0\Sigma^0\sigma(\omega)} = \frac{2-\bar\sigma^*_\Sigma}{D_{S\Sigma^0}}\, g_{\Sigma\Sigma\sigma(\omega)}. \tag{34}$$

$$g^*_{\Sigma^0\Sigma^0\sigma^*(\phi)} = \frac{2-(1/2)\,\bar\sigma_\Sigma}{D_{S\Sigma^0}}\, g_{\Sigma\Sigma\sigma^*(\phi)}. \tag{35}$$

For charged Σs we have

$$g^*_{\Sigma^+\Sigma^+\sigma(\omega,\delta,\rho)} = \frac{2-\bar\sigma^*_\Sigma}{D_{S\Sigma^+}}\, g_{\Sigma\Sigma\sigma(\omega,\delta,\rho)}, \tag{36}$$

$$g^*_{\Sigma^+\Sigma^+\sigma^*(\phi)} = \frac{2-(1/2)\left(\bar\sigma_\Sigma + \bar\delta_\Sigma\right)}{D_{S\Sigma^+}}\, g_{\Sigma\Sigma\sigma^*(\phi)}, \tag{37}$$

$$g^*_{\Sigma^-\Sigma^-\sigma(\omega,\delta,\rho)} = \frac{2-\bar\sigma^*_\Sigma}{D_{S\Sigma^-}}\, g_{\Sigma\Sigma\sigma(\omega,\delta,\rho)}, \tag{38}$$

$$g^*_{\Sigma^-\Sigma^-\sigma^*(\phi)} = \frac{2-(1/2)\left(\bar{\sigma}_\Sigma - \bar{\delta}_\Sigma\right)}{D_{S\Sigma^-}}\, g_{\Sigma\Sigma\sigma^*(\phi)}. \tag{39}$$

The renormalized meson-Ξ coupling constants are

$$g^*_{\Xi^0\Xi^0\sigma(\omega,\delta,\rho)} = \frac{2-(1/2)\,\bar{\sigma}^*_\Xi}{D_{S\Xi^0}}\, g_{\Xi\Xi\sigma(\omega,\delta,\rho)}, \tag{40}$$

$$g^*_{\Xi^0\Xi^0\sigma^*(\phi)} = \frac{2-\left(\bar{\sigma}_\Xi + \bar{\delta}_\Xi\right)}{D_{S\Xi^0}}\, g_{\Xi\Xi\sigma^*(\phi)}, \tag{41}$$

$$g^*_{\Xi^-\Xi^-\sigma(\omega,\delta,\rho)} = \frac{2-(1/2)\,\bar{\sigma}^*_\Xi}{D_{S\Xi^-}}\, g_{\Xi\Xi\sigma(\omega,\delta,\rho)}, \tag{42}$$

$$g^*_{\Xi^-\Xi^-\sigma^*(\phi)} = \frac{2-\left(\bar{\sigma}_\Xi - \bar{\delta}_\Xi\right)}{D_{S\Xi^-}}\, g_{\Xi\Xi\sigma^*(\phi)}. \tag{43}$$

Because $\bar{\sigma}_Y$, $\bar{\delta}_Y$ and $\bar{\sigma}^*_Y$ are expressed by m^*_p, m^*_n and m^*_Λ, the renormalized coupling constants (31)-(43) are also expressed by them.

Then, the three independent effective masses m^*_p, m^*_n and m^*_Λ, and the three independent vector potentials V_{0p}, V_{0n} and $V_{0\Lambda}$ are determined from extremizing the energy density (2) by them:

$$\begin{aligned} &C_{VN}\rho_p + \sum_{Y\neq\Lambda}\left(g^*_{nn\rho}\, g^*_{YY\omega} + g^*_{nn\omega}\, g^*_{YY\rho} I_{3Y} - C_{V\Lambda} g^*_{nn\rho}\, g^*_{YY\phi}\right)\rho_Y \\ &\quad - m^2_\omega\, g^*_{nn\rho}\,\langle\omega_0\rangle - m^2_\rho\, g^*_{nn\omega}\,\langle\rho_{03}\rangle + C_{V\Lambda} m^2_\phi\, g^*_{nn\rho}\,\langle\phi_0\rangle = 0, \end{aligned} \tag{44}$$

$$\begin{aligned} &C_{VN}\rho_n + \sum_{Y\neq\Lambda}\left(g^*_{pp\rho}\, g^*_{YY\omega} - g^*_{pp\omega}\, g^*_{YY\rho} I_{3Y} - C_{V\Lambda} g^*_{pp\rho}\, g^*_{YY\phi}\right)\rho_Y \\ &\quad - m^2_\omega\, g^*_{pp\rho}\,\langle\omega_0\rangle + m^2_\rho\, g^*_{pp\omega}\,\langle\rho_{03}\rangle + C_{V\Lambda} m^2_\phi\, g^*_{pp\rho}\,\langle\phi_0\rangle = 0, \end{aligned} \tag{45}$$

$$\sum_Y g^*_{YY\phi}\,\rho_Y - m^2_\phi\,\langle\phi_0\rangle = 0, \tag{46}$$

$$\begin{aligned} &\rho_{Sp} + \sum_{Y\neq\Lambda}\frac{\partial m^*_Y}{\partial m^*_p} M_Y \rho_{SY} + \sum_{Y\neq\Lambda}\frac{\partial V_Y}{\partial M^*_p} M_N \rho_Y + m^2_\sigma\,\langle\sigma\rangle\,\frac{\partial\langle\sigma\rangle}{\partial m^*_p} + m^2_\delta\,\langle\delta_3\rangle\,\frac{\partial\langle\delta_3\rangle}{\partial m^*_p} \\ &\quad + m^2_{\sigma^*}\,\langle\sigma^*\rangle\,\frac{\partial\langle\sigma^*\rangle}{\partial m^*_p} - m^2_\omega\,\langle\omega_0\rangle\,\frac{\partial\langle\omega_0\rangle}{\partial m^*_p} - m^2_\rho\,\langle\rho_{03}\rangle\,\frac{\partial\langle\rho_{03}\rangle}{\partial m^*_p} - m^2_\phi\,\langle\phi_0\rangle\,\frac{\partial\langle\phi_0\rangle}{\partial m^*_p} = 0, \end{aligned} \tag{47}$$

$$\begin{aligned} &\rho_{Sn} + \sum_{Y\neq\Lambda}\frac{\partial m^*_Y}{\partial m^*_n} M_Y \rho_{SY} + \sum_{Y\neq\Lambda}\frac{\partial V_Y}{\partial M^*_n} M_N \rho_Y + m^2_\sigma\,\langle\sigma\rangle\,\frac{\partial\langle\sigma\rangle}{\partial m^*_n} + m^2_\delta\,\langle\delta_3\rangle\,\frac{\partial\langle\delta_3\rangle}{\partial m^*_n} \\ &\quad + m^2_{\sigma^*}\,\langle\sigma^*\rangle\,\frac{\partial\langle\sigma^*\rangle}{\partial m^*_n} - m^2_\omega\,\langle\omega_0\rangle\,\frac{\partial\langle\omega_0\rangle}{\partial m^*_n} - m^2_\rho\,\langle\rho_{03}\rangle\,\frac{\partial\langle\rho_{03}\rangle}{\partial m^*_n} - m^2_\phi\,\langle\phi_0\rangle\,\frac{\partial\langle\phi_0\rangle}{\partial m^*_n} = 0, \end{aligned} \tag{48}$$

$$\sum_Y \frac{\partial m_Y^*}{\partial m_\Lambda^*} M_Y \rho_{SY} + \sum_{Y\neq\Lambda} \frac{\partial V_Y}{\partial M_\Lambda^*} M_\Lambda \rho_Y + m_{\sigma^*}^2 \langle\sigma^*\rangle \frac{\partial \langle\sigma^*\rangle}{\partial m_\Lambda^*} - m_\phi^2 \langle\phi_0\rangle \frac{\partial \langle\phi_0\rangle}{\partial m_\Lambda^*} = 0, \tag{49}$$

where $C_{V\Lambda} = g^*_{\Lambda\Lambda\omega}/g^*_{\Lambda\Lambda\phi}$. We omit the explicit expressions of the derivatives in the above equations because their derivations are tedious but straightforward tasks.

3 Numerical analyses

The present work investigates the cold β-equilibrated NS. The baryon and scalar densities in Eqs. (44)-(49) are determined from the chemical potentials μ_B through the Fermi momentum k_{FB}:

$$\mu_B = \left(k_{FB}^2 + M_B^{*\,2}\right)^{1/2} + V_{0B}. \tag{50}$$

The β-equilibrium condition requires

$$\mu_i = b_i\,\mu_n - q_i\,\mu_e, \tag{51}$$

where μ_i is the chemical potential of all the baryons and leptons, and b_i and q_i are the corresponding baryon number and charge. There exist only two independent chemical potentials of neutron and electron. They are determined so as to satisfy the baryon number conservation

$$\rho_T = \sum_{\substack{B=p,n,\Lambda,\Sigma^+,\\ \Sigma^0,\Sigma^-,\Xi^0,\Xi^+}} \rho_B, \tag{52}$$

and the charge neutral condition

$$\sum_{i=B,l} q_i\,\rho_i = 0. \tag{53}$$

We solve nonlinear simultaneous equations (44)-(49), (52) and (53) for a given value of ρ_T by means of the 8-rank Newton-Raphson method.

For calculating in RMF model, we have to specify the meson-baryon coupling constants. The $NN\sigma$ and $NN\omega$ coupling constants, $\left(g_{NN\sigma}/m_\sigma\right)^2 = 16.9\,\mathrm{fm}^2$ and $\left(g_{NN\omega}/m_\omega\right)^2 = 12.5\,\mathrm{fm}^2$, have been determined [18] so as to reproduce the nuclear matter saturation energy $-15.75\,\mathrm{MeV}$ at the saturation density $0.16\,\mathrm{fm}^{-3}$. The resultant effective nucleon mass and the incompressibility of saturated nuclear matter are $m_N^* = 0.605$ and $K = 302\,\mathrm{MeV}$. The $NN\delta$ coupling constant $\left(g_{NN\delta}/m_\delta\right)^2 = 0.39\,\mathrm{fm}^2$ is assumed to be the same as the Bonn A potential in Ref. [29]. On the other hand, the $NN\rho$ coupling constant $(g_{NN\rho}/m_\rho)^2 = 1.433\,\mathrm{fm}^2$ is determined so as to reproduce the empirical symmetry energy of nuclear matter $E_s = 32.0\,\mathrm{MeV}$ [30].

Next, the meson-hyperon coupling constants have to be determined. Unfortunately, at present, there is little reliable information on the nucleon-hyperon (NY) and the hyperon-hyperon (YY) interactions. In this work we will investigate the two sets of the coupling constants. First, all the meson-hyperon coupling constants are related to the meson-

Table 1: The two sets of meson-hyperon coupling constants used in the calculations of NS matter.

Coupling constants	EZM-SU6	EZM-P
$g_{\Lambda\Lambda\omega}$	$(2/3)\, g_{NN\omega}$	
$g_{\Sigma\Sigma\omega}$	$(2/3)\, g_{NN\omega}$	
$g_{\Xi\Xi\omega}$	$(1/3)\, g_{NN\omega}$	
$g_{\Lambda\Lambda\sigma}$	$(2/3)\, g_{NN\sigma}$	$0.604\, g_{NN\sigma}$
$g_{\Sigma\Sigma\sigma}$	$(2/3)\, g_{NN\sigma}$	$0.461\, g_{NN\sigma}$
$g_{\Xi\Xi\sigma}$	$(1/3)\, g_{NN\sigma}$	$0.309\, g_{NN\sigma}$
$g_{\Lambda\Lambda\phi}$	$-(\sqrt{2}/3)\, g_{NN\omega}$	
$g_{\Sigma\Sigma\phi}$	$-(\sqrt{2}/3)\, g_{NN\omega}$	
$g_{\Xi\Xi\phi}$	$-(2\sqrt{2}/3)\, g_{NN\omega}$	
$g_{\Lambda\Lambda\sigma^*}$	$(\sqrt{2}/3)\, g_{NN\sigma}$	$0.558\, g_{NN\sigma}$
$g_{\Sigma\Sigma\sigma^*}$	$(\sqrt{2}/3)\, g_{NN\sigma}$	$0.558\, g_{NN\sigma}$
$g_{\Xi\Xi\sigma^*}$	$(2\sqrt{2}/3)\, g_{NN\sigma}$	$1.128\, g_{NN\sigma}$
$g_{\Sigma\Sigma\rho}$	$2\, g_{NN\rho}$	
$g_{\Xi\Xi\rho}$	$g_{NN\rho}$	
$g_{\Sigma\Sigma\delta}$	$2\, g_{NN\delta}$	
$g_{\Xi\Xi\delta}$	$g_{NN\delta}$	

nucleon coupling constants through the SU(6) symmetry. Hereafter the result using this set will be referred as EZM-SU6. Because the EZM model is based on the constituent quark model, this set seems to be consistent to the model. However, the NY interactions from the SU(6) symmetry become too attractive to be consistent with the existing data of hypernuclei. Especially, no observation of Σ hypernuclei strongly suggests the repulsive $N\Sigma$ potential. In addition the detailed theoretical analyses of Σ^- atomic data [31] and (π^-, K^+) inclusive spectra [32,33] predict a repulsive Σ-nucleus optical potential in the nuclear interior.

Another set of the coupling constants is determined in a phenomenological way together with the SU(6) symmetry. First, the $YY\omega$, $YY\delta$, $YY\rho$ and $YY\phi$ coupling constants are determined through the SU(6) symmetry. Then, the $YY\sigma$ coupling constants are determined [11,34] so as to reproduce the empirical hyperon potentials in saturated nuclear matter of the density $\rho_{nm} = 0.16\,\mathrm{fm}^{-3}$:

$$U_\Lambda^{(N)}(\rho_{nm}) = -28\,\mathrm{MeV}, \quad U_\Sigma^{(N)}(\rho_{nm}) = 30\,\mathrm{MeV}, \quad U_\Xi^{(N)}(\rho_{nm}) = -18\,\mathrm{MeV}, \tag{54}$$

where $U_B^{(B')}\left(\rho_{B'}\right)$ is the potential of a single baryon B embedded in a bath of baryon B' with density $\rho_{B'}$. The $YY\sigma$ coupling constants from Eq. (54) are the most plausible at present.

Next, the $YY\sigma^*$ coupling constants are adjusted [35] so that the potential of a single

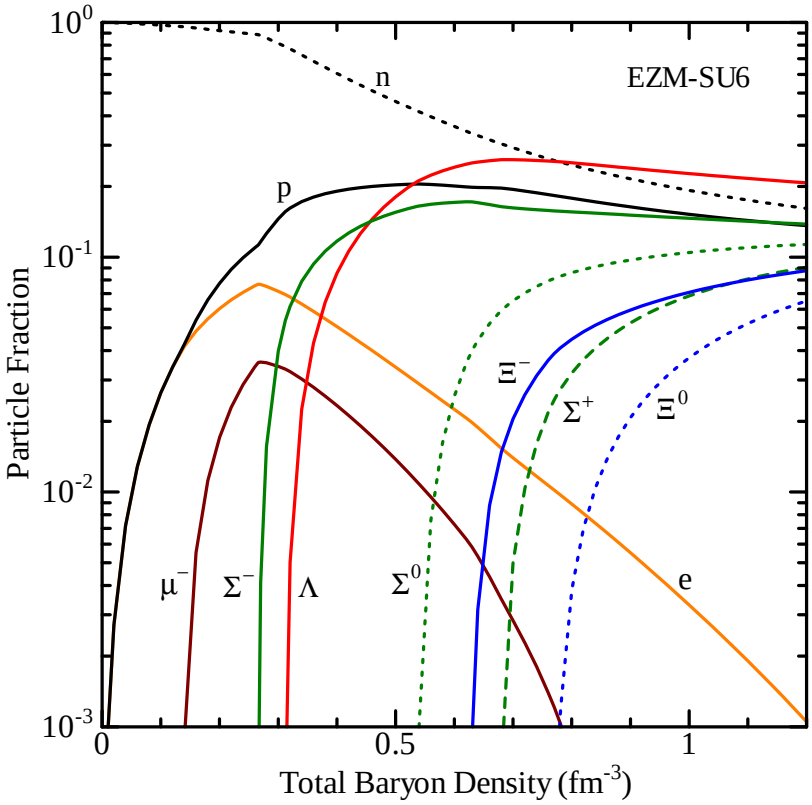

Figure 1: The particle fractions in NS as functions of the total baryon density using the EZM-SU6 coupling set.

hyperon, embedded in a bath of Ξ matter at ρ_{nm}, becomes

$$U_{\Xi}^{(\Xi)}(\rho_{nm}) = U_{\Lambda}^{(\Xi)}(\rho_{nm}) = -10\,\mathrm{MeV}. \tag{55}$$

The resultant coupling constants predict a weak attractive $\Lambda\Lambda$ interaction, which is consistent to the recent data [36] of ${}^{\ 6}_{\Lambda\Lambda}\mathrm{He}$. Hereafter the result using this second set of the coupling constants will be referred as EZM-P. The values of meson-hyperon coupling constants of each set are summarized in Table I.

Using the above two sets of meson-baryon coupling constants, we calculate the properties of the cold NS matter. There are the upper limits of the total baryon densities, $\rho_T = 1.202\,\mathrm{fm}^{-3}$ and $1.706\,\mathrm{fm}^{-3}$ for EZM-SU6 and EZM-P, above which an effective mass of one baryon becomes negative. However, in contrast to Ref. [23] we do not encounter before the negative mass the upper limits of the densities, above which there are no β-equilibrium states. In Ref. [23] we first solved Eqs. (44)-(46) so as to obtain the explicit expressions for the three independent vector potentials of p, n and Λ. Then, they were substituted into Eqs. (47)-(49). As well as the resultant set of nonlinear equations we have another set of equations (52) and (53). Because Eq. (50) determining the baryon densities contains the vector potentials, the two sets of nonlinear equations were solved consistently but independently by means of iteration. To the contrary, if we treat the

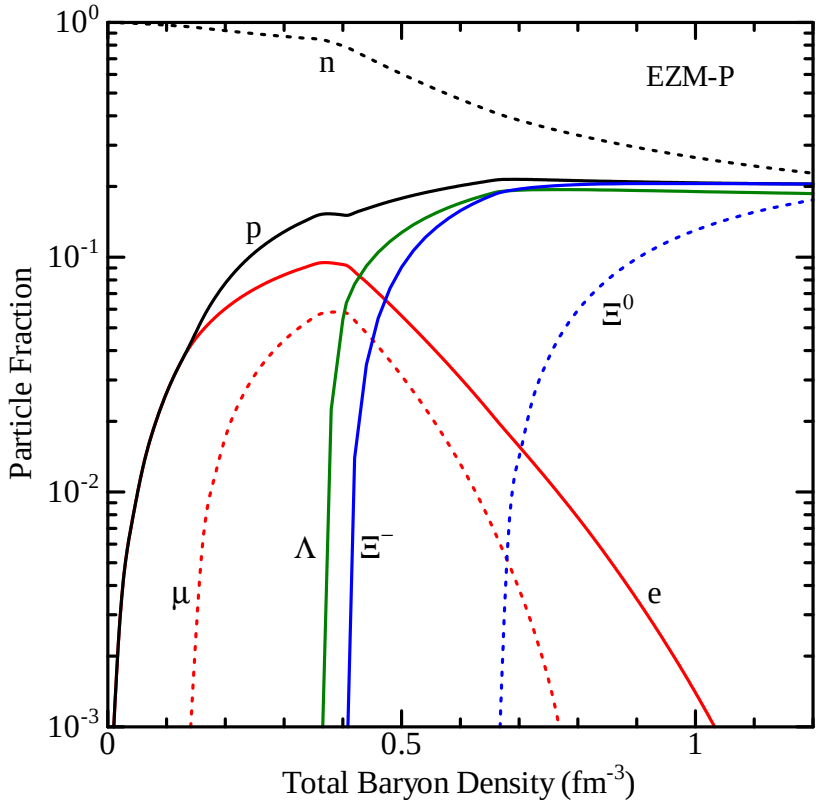

Figure 2: The same as Figure 1 but for the EZM-P coupling set.

vector potentials on an equal footing with the effective masses, the 8 nonlinear equations (44)-(49), (52) and (53) can be solved simultaneously. The present work has adopted this method.

Figures 1 and 2 show the particle fractions in NS as functions of the total baryon density using the two sets of meson-baryon couplings, respectively. Due to the attractive $N\Sigma$ interaction the Σ hyperons are abundant in the EZM-SU6. The Σ^- appears earlier than Λ because of its negative charge. To the contrary, the Σs appear above $\rho_T = 1.5\,\mathrm{fm}^{-3}$ in the EZM-P. On the other hand, due to the baryon number conservation the Ξ hyperons appear earlier and are more abundant in the EZM-P than the EZM-SU6.

Figure 3 shows the EOSs of NS matter using the EZM-P (the solid curve) and the EZM-SU6 (the dashed curve). The pressure is calculated by means of the Gibbs-Duhem relation $P = \mu_n \rho_T - \mathcal{E}$. The kinks in the curves correspond to the appearances of hyperons. Due to the early appearance of Σ^- the EZM-SU6 is softer than the EZM-P in the region of $250\,\mathrm{MeV{\cdot}fm}^{-3} < \mathcal{E} < 800\,\mathrm{MeV{\cdot}fm}^{-3}$. It is therefore expected that the difference in the two models is revealed for low-mass NSs as in J0737-3039. We will tabulate our EOSs in the appendix.

In Figure 4 we calculate the mass sequence of non-rotating NSs by integrating the

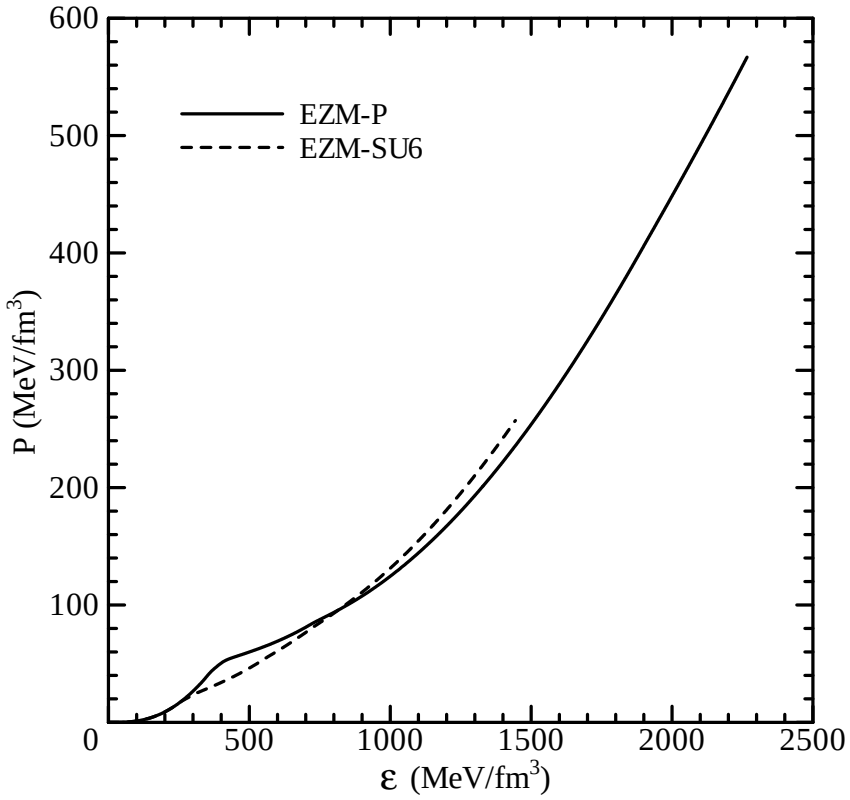

Figure 3: The EOSs of cold non-rotating NS matter using the two sets of meson-baryon coupling constants.

Tolman-Oppenheimer-Volkov (TOV) equation [37].

$$\frac{d\,M\,(r)}{d\,r} = \frac{4\pi^2}{c^2}\,r^2\,\mathcal{E}\,(r)\,, \tag{56}$$

$$\frac{d\,P\,(r)}{d\,r} = -\,\frac{G}{c^2}\,\frac{[\,\mathcal{E}(r) + P\,(r)\,]\left[M\,(r) + 4\pi r^3 P\,(r)/c^2\right]}{r\left[r - 2\,GM\,(r)/c^2\right]}, \tag{57}$$

where $P\,(r)$, $\mathcal{E}\,(r)$ and $M\,(r)$ are the radial distributions of pressure, energy and mass of NS. The EOSs from the EZM models are for the high-density core-region of NS. For the outer region below $\rho_T = 0.1\mathrm{fm}^{-3}$, we employ the EOSs by Feynman-Metropolis-Teller, Baym-Pethick-Sutherland and Negele-Vautherin in Ref. [38]. The maximum gravitational masses of NSs in the EZM-SU6 and EZM-P are $1.353M_\odot$ and $1.566M_\odot$, respectively. The former appears just on the upper limit of ρ_T and exceeds barely the masses of NSs in J0737-3039. The EZM-SU6 however cannot reproduce the famous canonical value $1.441M_\odot$ of the relativistic binary pulsar B1913+16 [39], while the EZM-P reproduces the most massive NS PSR J1518+4904 residing in the six known binary radio pulsar systems [40] that provide NSs with the most accurately determined masses. This is due to the soft EOS of EZM-SU6 in the medium-density region. It is remarkable that in the EZM-P the radii of all the NSs are larger than 13 km. Especially, the radius

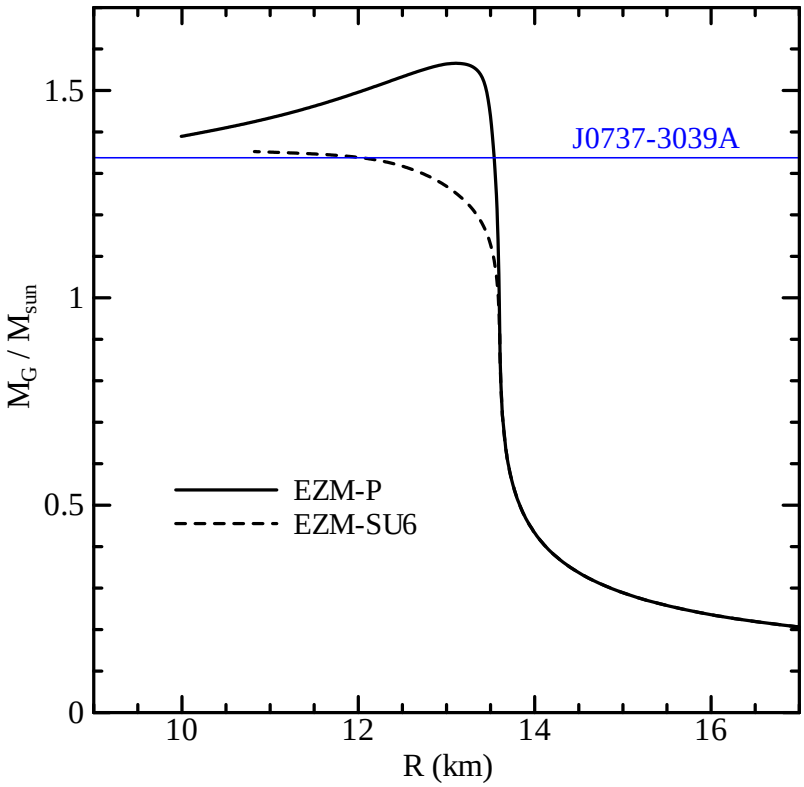

Figure 4: The mass-radius relation of NSs using the EOSs from the two EZM models. The blue holizontal line indicates the gravitational mass of J0737-3039A.

remains approximately constant for $M_G \geq 0.5 M_\odot$. On the other hand, the EZM-SU6 predicts smaller radii of NSs with $M_G > M_\odot$. Among the mass-radius relations of the various modern EOSs presented in Fig. 7 of Ref. [41], only the EOS labeled "MS0" predicts larger radii than 13 km for all the NSs. However, the MS0 [10] takes into account nucleons only and predicts a larger radius of NS with $M_G = 1.4 M_\odot$ than the upper limit $R = 14.4$ km derived recently from J1748+2446ad [42]. We can therefore see that the EZM-P has a unique feature in all the models of dense nuclear matter.

According to the suggestions in Refs. [7-9] we next investigate the moment-of-inertia I of J0737-3039A. Under the slow-rotation approximation [7,37,43] it is calculated by a numerical quadrature:

$$I = \frac{8\pi}{3} \frac{G}{c^4} \int_0^R dr\, r^4 \frac{[\,\mathcal{E}(r) + P(r)\,]\, e^{-\Phi(r)}}{\left(1 - \frac{2GM(r)}{c^2\, r}\right)^{1/2}} \frac{\bar{\omega}(r)}{\Omega}, \tag{58}$$

where R is the NS radius and Ω is the observed stellar rotational frequency. The quantities $\bar{\omega}(r)$ and $\Phi(r)$ are calculated by integrating the following differential equations together

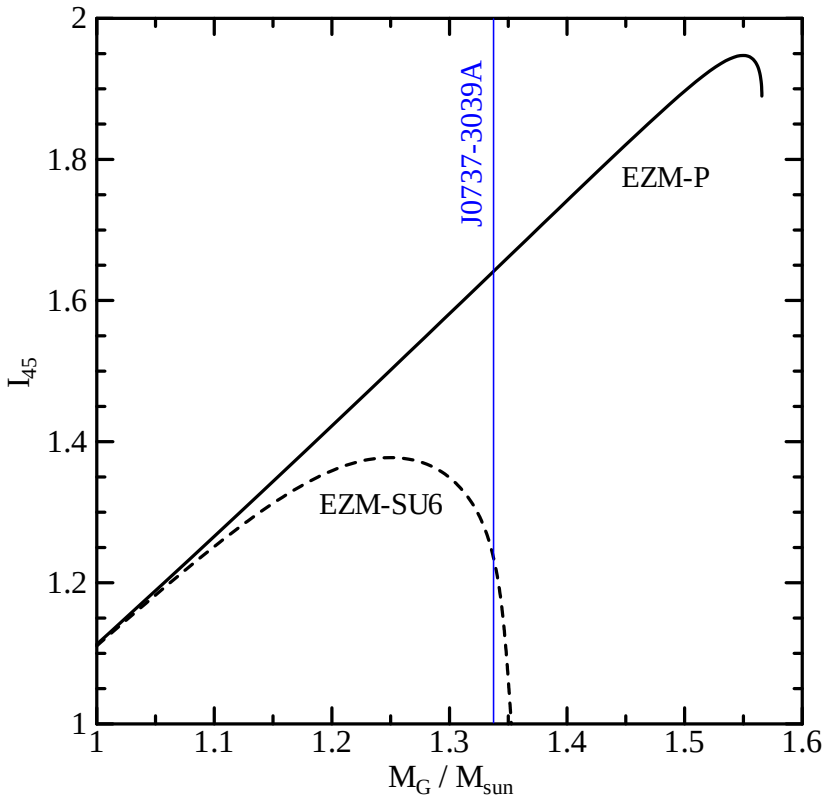

Figure 5: The NS moment-of-inertia $I_{45} \equiv I/10^{45}\mathrm{g{\cdot}cm^2}$ with angular velocity $\Omega = 276.8\,\mathrm{s}^{-1}$ as functions of the gravitational mass. The solid and dashed curves are the results of EZM-P and EZM-SU6, respectively. The blue vertical line indicates the gravitational mass of J0737-3039A.

with the TOV equations (56) and (57):

$$\frac{d\Phi(r)}{dr} = -\frac{1}{\mathcal{E}\,(r) + P(r)}\frac{dP(r)}{dr}, \tag{59}$$

$$\frac{1}{r^3}\frac{d}{dr}\left(r^4 j(r)\,\frac{d\,\bar{\omega}(r)}{dr}\right) + 4\,\bar{\omega}(r)\,\frac{d\,j(r)}{dr} = 0, \tag{60}$$

where

$$j(r) = \left(1 - \frac{2GM(r)}{c^2\,r}\right)^{1/2} e^{-\Phi(r)}. \tag{61}$$

Figure 5 shows the moments-of-inertia $I_{45} \equiv I/10^{45}\mathrm{g{\cdot}cm^2}$ with angular velocity $\Omega = 276.8\,\mathrm{s}^{-1}$ as functions of the gravitational mass. They increase linearly as long as the radius remains approximately constant. The linearity is prominent in the EZM-P below $M_G = 1.5M_\odot$. After the maximum value $I_{45} = 1.95$ with $M_G = 1.55M_\odot$ in the EZM-P and $I_{45} = 1.38$ with $M_G = 1.25M_\odot$ in the EZM-SU6 they turn to decrease. The phenomenon is striking in the EZM-SU6 because the radius decreases rapidly above $M_G = 1.3M_\odot$. For J0737-3039A we find $I_{45} = 1.64$ with the radius $R = 13.54\,\mathrm{km}$ in the EZM-P and $I_{45} = 1.23$ with $R = 12.03\,\mathrm{km}$ in the EZM-SU6. Another remarkable difference in the

two models is the central baryon density of J0737-3039A. Its value in the EZM-P is $\rho_C = 0.352\,\mathrm{fm}^{-3}$, which is somewhat lower than the threshold $\rho_T = 0.36\,\mathrm{fm}^{-3}$ of Λ. To the contrary, the central baryon density in the EZM-SU6 is $\rho_C = 0.844\,\mathrm{fm}^{-3}$, which is higher than $\rho_C = 0.670\,\mathrm{fm}^{-3}$ of the most massive NS in the EZM-P. The J0737-3039A is composed of only nucleons in the EZM-P, while it contains all the baryon octets in the EZM-SU6.

Then, compared with Table 1 in Ref. [7] the moment-of-inertia in the EZM-SU6 is found to be nearly equal to $I_{45} = 1.24$ in the EOS labeled "APR" [44]. However, the mass-radius relations in both the EOSs are quite different from each other. On the other hand, the moment-of-inertia in the EZM-P is close to $I_{45} = 1.66$ in the EOS labeled "MS1" [10]. However, the radius of the most massive NS is $R = 13.1\,\mathrm{km}$ in the former but is smaller than $R = 12\,\mathrm{km}$ in the latter. In the comparison with Table 1 in Ref. [8] we find that the EZM-P perfectly agrees with the empirical EOS labeled "BGN2H1" [45]. This is reasonable because both the EOSs are relatively stiff and take into account Λ and Ξ hyperons. However, the BGN2H1 predicts the most massive NS being heavier than $M_G = 1.8 M_\odot$.

The above results indicate that the EOSs in the EZM models have quite unique nature and so are clearly different from the other EOSs. In fact, our results fill in the blank on the correlation map of Fig. 3 in Ref. [8] between the NS maximum mass and the J0737-3039A moment-of-inertia presented for 25 EOSs in all. Therefore, the expected measurement of the moment-of-inertia has a serious effect on the EZM model. If $I_{45} \approx 1.2$ should be proved, the present EZM model is ruled out because the EZM-SU6 cannot reproduce the canonical NS mass $M_G = 1.441 M_\odot$. In this case the nuclear matter should be much softer [1] than $K \simeq 300\,\mathrm{MeV}$ in the EZM model. The observations [2,3,46] suggesting the soft EOS should be also rejected. However, the EOS by APR [44] is not readily supported because its moment-of-inertia becomes smaller than $I_{45} \approx 1.2$ if the hyperons are taken into account.

Inversely, if $I_{45} \approx 1.6$ is proved, the EZM model turns out to be a physically reasonable model of dense baryon matter because it naturally rejects the unphysical strong NY attractive interactions in the EZM-SU6 that leads to the unphysical small moment-of-inertia $I_{45} \approx 1.2$. Nevertheless, the EZM model still has problems because the EZM-P cannot reproduce the recently observed massive NS [47] and the redshift [48] of EXO 0748-676. This indicates that the YY interactions in the EZM-P should be largely modified. In fact, the $YY\sigma^*$ coupling set 4 in Ref. [23], which is somewhat different from the EZM-P, merely produces the almost the same results as the EZM-P, while the EZM model without hyperons [13] is satisfactory. Even if we construct a hybrid model, in which the $YY\sigma$ coupling constants are the same as EZM-P while the $YY\sigma^*$ coupling constants are the same as EZM-SU6, the most massive NS with $M_G = 1.67 M_\odot$ and $R = 12.6\,\mathrm{km}$ cannot yet reproduce the observations in Refs. [47,48]. It is however noted that the artificial adjustment of the coupling constants as in the recent work [49] has no physical meanings.

Finally, we have to mention the results of Ref. [23], in which four sets of meson-hyperon coupling constants were considered. Are they revised in the new calculus of NS matter developed in the present work? Of course, the new calculus provide the same results as the old one in Ref. [23] below the upper limits of β-equilibrium states. Thus, there is no physical revision in the result using the set 4 of coupling constants because the central baryon density of the most massive NS was lower than the upper limit. Moreover, the set 2 remains to be invalid because the unphysical behavior of EOS occurred far below the upper limit. To the contrary, the result using the set 1 is slightly revised. In the new calculus we can find the most massive NS above the upper limit in Ref. [23]. However, the mass is still lower than the canonical value $M_G = 1.441 M_\odot$. For the set 3 in the new calculus we can also find the most massive NS. However, above its central density there appears an unphysical behavior of EOS as in the set 2. Consequently, we can conclude that the essential results of Ref. [23] are still valid.

4 Summary

We revisit the EZM model of dense NS core matter. In our previous work we solved a set of equations to determine the effective masses of strongly interacting baryons in dense baryon matter consistently but independently together with a set of equations to determine the conditions of β-equilibrated NS matter. There we encountered an upper limit of the total baryon density above which no β-equilibrium states were found. In the present work this problem has been resolved by treating the vector potentials of baryons on an equal footing with the effective masses. The 8 nonlinear equations (44)-(49), (52) and (53) are solved simultaneously using 8-rank Newton-Raphson method. Nevertheless, we want to emphasize that the essential results and conclusions in Ref. [23] are still valid.

We have investigated the two sets of hyperon coupling constants, EZM-SU6 and EZM-P. The former is due to SU(6) symmetry while the latter is derived from the empirical data of hypernuclei. There are still the upper limits of the density above which an effective mass of one baryon becomes negative. This problem is intrinsic to all the RMF models. It is a crucial issue to the EZM-SU6 where the maximum gravitational mass of NS is lower than the canonical value $1.441 M_\odot$, while it does not bother the EZM-P where the central baryon density in NS of the maximum mass is lower than the upper limit.

Next, inspired by an expectation that the precisely measurable moment-of-inertia of J0737-3039A will be able to constrain the nuclear EOS severely, we calculate it in the EZM models using Hartle's slow-rotation approximation. We find $I_{45} = 1.23$ and 1.64 in EZM-SU6 and EZM-P, respectively. Compared with the result of Ref. [7], the former is close to the value in the EOS of "APR", while the latter approximately equals to the value in the EOS of "MS1". However, their mass-radius relations of NS are rather different from the EZM models. Moreover, the EZM models fill in the blank on the correlation map in Ref. [8] between the maximum gravitational mass of NS and the moment-of-inertia of

J0737-3039A for many other EOSs.

Consequently, we have found that the EZM models have quite unique features being different from the other EOSs. This implies that the moment-of-inertia of J0737-3039A impose a severe test on the EZM model. However, whether $I_{45} \approx 1.2$ or 1.6 will be proved, there still remain the problems in the nuclear EOS, especially about the strange contents of NS matter. In this respect our future work will investigate the quark matter core in NS within the EZM model.

Appendix: Table of the EOSs

For the reproduction of our results we here tabulate the EOSs, the pressure P vs. the baryon density ρ_T and the energy density $\mathcal{E}$, of the EZM models in the core region $0.08\,\mathrm{fm}^{-3} \leq \rho_T \leq 1.20\,\mathrm{fm}^{-3}$ of NSs. For the crust we have used the EOSs in Ref. [38].

	EZM-SU6		EZM-P	
$\rho_T(\mathrm{cm}^{-3})$	$\mathcal{E}(\mathrm{g}\cdot\mathrm{cm}^{-3})$	$P(\mathrm{dyn}\cdot\mathrm{cm}^{-2})$	$\mathcal{E}(\mathrm{g}\cdot\mathrm{cm}^{-3})$	$P(\mathrm{dyn}\cdot\mathrm{cm}^{-2})$
8.00E+37	1.347325E+14	7.471047E+32	1.347325E+14	7.471048E+32
1.00E+38	1.687169E+14	1.542228E+33	1.687169E+14	1.542228E+33
1.20E+38	2.029225E+14	2.763049E+33	2.029225E+14	2.763049E+33
1.40E+38	2.373981E+14	4.468760E+33	2.373981E+14	4.468760E+33
1.60E+38	2.721813E+14	6.653920E+33	2.721813E+14	6.653920E+33
1.80E+38	3.073065E+14	9.410092E+33	3.073065E+14	9.410092E+33
2.00E+38	3.428106E+14	1.280365E+34	3.428106E+14	1.280365E+34
2.20E+38	3.787297E+14	1.689086E+34	3.787297E+14	1.689086E+34
2.40E+38	4.150990E+14	2.172127E+34	4.150990E+14	2.172127E+34
2.60E+38	4.519518E+14	2.733817E+34	4.519518E+14	2.733817E+34
2.80E+38	4.892745E+14	3.210948E+34	4.893200E+14	3.377866E+34
3.00E+38	5.269368E+14	3.633898E+34	5.272335E+14	4.107359E+34
3.20E+38	5.649225E+14	4.057874E+34	5.657202E+14	4.924762E+34
3.40E+38	6.032022E+14	4.415922E+34	6.048062E+14	5.831936E+34
3.60E+38	6.417722E+14	4.769202E+34	6.445155E+14	6.826471E+34
3.80E+38	6.806488E+14	5.132332E+34	6.848203E+14	7.607459E+34
4.00E+38	7.198526E+14	5.512048E+34	7.256889E+14	8.272574E+34
4.20E+38	7.594060E+14	5.912693E+34	7.671369E+14	8.699069E+34
4.40E+38	7.993309E+14	6.337615E+34	8.089685E+14	9.008271E+34
4.60E+38	8.396485E+14	6.789683E+34	8.511292E+14	9.312604E+34
4.80E+38	8.803787E+14	7.271513E+34	8.936116E+14	9.624756E+34
5.00E+38	9.215393E+14	7.785569E+34	9.364142E+14	9.951342E+34
5.20E+38	9.631459E+14	8.334204E+34	9.795375E+14	1.029701E+35
5.40E+38	1.005205E+15	8.908970E+34	1.022983E+15	1.066548E+35
5.60E+38	1.047661E+15	9.460620E+34	1.066752E+15	1.105996E+35
5.80E+38	1.090506E+15	1.002570E+35	1.110848E+15	1.148328E+35
6.00E+38	1.133735E+15	1.061737E+35	1.155271E+15	1.193800E+35
6.20E+38	1.177348E+15	1.124231E+35	1.200025E+15	1.242647E+35

continued

	EZM-SU6		EZM-P	
$\rho_T(\mathrm{cm}^{-3})$	$\mathcal{E}(\mathrm{g}\cdot\mathrm{cm}^{-3})$	$P(\mathrm{dyn}\cdot\mathrm{cm}^{-2})$	$\mathcal{E}(\mathrm{g}\cdot\mathrm{cm}^{-3})$	$P(\mathrm{dyn}\cdot\mathrm{cm}^{-2})$
6.40E+38	1.221376E+15	1.188151E+35	1.245110E+15	1.295082E+35
6.60E+38	1.265794E+15	1.254042E+35	1.290529E+15	1.351299E+35
6.80E+38	1.310563E+15	1.322127E+35	1.336316E+15	1.402747E+35
7.00E+38	1.355611E+15	1.386781E+35	1.382404E+15	1.452648E+35
7.20E+38	1.400942E+15	1.452809E+35	1.428756E+15	1.504423E+35
7.40E+38	1.446557E+15	1.521535E+35	1.475365E+15	1.558850E+35
7.60E+38	1.492455E+15	1.593523E+35	1.522226E+15	1.616342E+35
7.80E+38	1.538649E+15	1.668010E+35	1.569338E+15	1.677180E+35
8.00E+38	1.585138E+15	1.744593E+35	1.616699E+15	1.741585E+35
8.20E+38	1.631909E+15	1.824464E+35	1.664311E+15	1.809764E+35
8.40E+38	1.678958E+15	1.907947E+35	1.712171E+15	1.882008E+35
8.60E+38	1.726285E+15	1.995234E+35	1.760288E+15	1.958137E+35
8.80E+38	1.773889E+15	2.086468E+35	1.808665E+15	2.038161E+35
9.00E+38	1.821769E+15	2.181802E+35	1.857303E+15	2.122177E+35
9.20E+38	1.869931E+15	2.281216E+35	1.906204E+15	2.210277E+35
9.40E+38	1.918374E+15	2.384746E+35	1.955370E+15	2.302542E+35
9.60E+38	1.967101E+15	2.492446E+35	2.004802E+15	2.399047E+35
9.80E+38	2.016113E+15	2.604365E+35	2.054503E+15	2.499861E+35
1.00E+39	2.065411E+15	2.720543E+35	2.104474E+15	2.605048E+35
1.02E+39	2.114996E+15	2.841013E+35	2.154717E+15	2.714663E+35
1.04E+39	2.164871E+15	2.965806E+35	2.205234E+15	2.828759E+35
1.06E+39	2.215035E+15	3.094945E+35	2.256028E+15	2.947381E+35
1.08E+39	2.265492E+15	3.228449E+35	2.307100E+15	3.070571E+35
1.10E+39	2.316241E+15	3.366333E+35	2.358453E+15	3.198365E+35
1.12E+39	2.367284E+15	3.508606E+35	2.410089E+15	3.330795E+35
1.14E+39	2.418623E+15	3.655273E+35	2.462010E+15	3.467887E+35
1.16E+39	2.470258E+15	3.806334E+35	2.514218E+15	3.609663E+35
1.18E+39	2.522192E+15	3.961782E+35	2.566716E+15	3.756143E+35
1.20E+39	2.574424E+15	4.121603E+35	2.619505E+15	3.907340E+35

References

[1] C. Sturm *et al.*, Phys. Rev. Lett. **86** (2001) 39 [arXiv:nucl-ex/0011001].

[2] T.M. Braje and R.W. Romani, Astrophys. J. **580** (2002) 1043.

[3] F. Őzel, arXiv:astro-ph/0605106.

[4] M. Burgay *et al.*, Nature **426** (2003) 531 [arXiv/astro-ph/0312071].

[5] A.G. Lyne *et al.*, Science **303** (2004) 1153 [arXiv:astro-ph/0401086].

[6] M. Kramer *et al.*, The 22nd Texas Symposium on Relativistic Astrophysics, 2004 [arXiv:astro-ph/0503386].

[7] I.A. Morrison, T.W. Baumgarte, S.L. Shapiro and V.R. Pandharipande, Astrophys. J. **617** (2004) L135 [arXiv:astro-ph/0411353].

[8] M. Bejger, T. Bulik and P. Haensel, Mon. Not. Roy. Astron. Soc. **364** (2005) 635 [arXiv:astro-ph/0508105].

[9] J.M. Lattimer and B.F. Schutz, Astrophys. J. **629** (2005) 979 [arXiv:astro-ph/0411470].

[10] H. Müller and B.D. Serot, Nucl. Phys. A **606** (1996) 508 [arXiv: nucl-th/9603037].

[11] N.K. Glendenning and S.A. Moszkowski, Phys. Rev. Lett. **67** (1991) 2414.

[12] T. Klähn *et al.*, arXiv:nucl-th/0602038.

[13] K. Miyazaki, Mathematical Physics Preprint Archive (mp_arc) 06-103.

[14] B.G. Todd-Rutel and J. Piekarewicz, Phys. Rev. Lett. **95** (2005) 122501 [arXiv:nucl-th/0504034].

[15] S. Typel, Phys. Rev. C **71** (2005) 064301 [arXiv:nucl-th/0501056].

[16] J. Zimanyi and S.A. Moszkowski, Phys. Rev. C **42** (1990) 1416.

[17] E.E. Kolomeitsev and D.N. Voskresensky, Nucl. Phys. A **759** (2005) 373 [arXiv:nucl-th/0410063].

[18] K. Miyazaki, Mathematical Physics Preprint Archive (mp_arc) 05-178.

[19] K. Miyazaki, Mathematical Physics Preprint Archive (mp_arc) 05-190.

[20] K. Miyazaki, Mathematical Physics Preprint Archive (mp_arc) 05-199.

[21] K. Miyazaki, Mathematical Physics Preprint Archive (mp_arc) 05-206.

[22] K. Miyazaki, Mathematical Physics Preprint Archive (mp_arc) 05-216.

[23] K. Miyazaki, Mathematical Physics Preprint Archive (mp_arc) 05-224.

[24] K. Miyazaki, Mathematical Physics Preprint Archive (mp_arc) 05-233.

[25] K. Miyazaki, Mathematical Physics Preprint Archive (mp_arc) 06-91.

[26] K. Miyazaki, Mathematical Physics Preprint Archive (mp_arc) 05-427.

[27] S. Kubis and M. Kutschera, Phys. Lett. B **399** (1997) 191, [arXiv:astro-ph/9703049].

[28] J. Schaffner, C.B. Dover, A. Gal, C. Greiner and H. Stőker, Phys. Rev. Lett. **71** (1993) 1328.

[29] R. Brockmann and R. Machleidt, Phys. Rev. C **42** (1990) 1965.

[30] B-A. Li, L-W. Chen, C.M. Ko, G-C. Yong and W. Zuo, arXiv:nucl-th/0504009; B-A. Li, L-W. Chen, C.M. Ko and A.W. Steiner, arXiv:nucl-th/0601028.

[31] J. Mareš, E. Friedman, A. Gal and B.K. Jennings, Nucl. Phys. A **594** (1995) 311 [arXiv:nucl-th/9505003].

[32] M. Kohno, Y. Fujiwara, Y. Watanabe, K. Ogata and M. Kawai, Prog. Theor. Phys. **112** (2004) 895 [arXiv:nucl-th/0410073].

[33] J. Dąbrowski and J. Rożynek, Acta Phys. Polon. B **37** (2006) 87.

[34] J. Schaffner-Bielich, M. Hanauske, H. Stőker and W. Greiner, Phys. Rev. Lett. **89** (2002) 171101, [arXiv:astro-ph/0005490].

[35] W.L. Qian, R.K. Su and H.Q. Song, J. Phys. G **30** (2004) 1893 [arXiv:nucl-th/0409063].

[36] H. Takahashi *et al.*, Phys. Rev. Lett. **87** (2001) 212502.

[37] W.D. Arnett and R.L. Bowers, Astrophys. J. Suppl. **33** (1977) 415.

[38] V. Canuto, Ann. Rev. Astr. Ap. **12** (1974) 167; **13** (1975) 335.

[39] J.M. Weisberg and J.H. Taylor, Proceedings of August 2002 meeting "Radio Pulsars" in Chania, Crete, ASP Conference Series Vol. CS-302 (2003), M. Bailes, D.J. Nice and S.E. Thorsett, eds. [arXiv:astro-ph/0211217].

[40] S.E. Thorsett and D. Chakrabarty, Astrophys. J. **512** (1999) 288.

[41] J.M. Lattimer and M. Prakash, Astrophys. J. **550** (2001) 426.

[42] J.W.T. Hessels *et al.*, arXiv:astro-ph/0601337.

[43] J.B. Hartle, Astrophys. J. **150** (1967) 1005.

[44] A. Akmal, V.R. Pandharipande and D.G. Ravenhall, Phys. Rev. C **58** (1998) 1804 [arXiv:nucl-th/9804027].

[45] S. Balberg, I. Lichtenstadt and G.B. Cook, Astrophys. J. Suppl. **121** (1999) 515

[46] M. Bejger and P. Haensel, Astron. Astrophys. **396** (2002) 917 [arXiv:astro-ph/0209151].

[47] S.M. Ransom *et al.*, Science **307** (2005) 892 [arXiv:astro-ph/0501230].

[48] J. Cottam, F. Paerels and M. Mendez, Nature **420** (2002) 51 [arXiv:astro-ph/0211126].

[49] B.D. Lackey, M. Nayyar and B.J. Owen, Phys. Rev. D **73** (2006) 024021 [arXiv:astro-ph/0507312].